

A New Control Architecture For Multi-Beam Fringe Tracker

L. Vincent^{a,b}, M. Alamir^a, J.B. Le Bouquin^c, K. Perraut^b, P. Kern^b, L. Jocou^b and J.P. Berger^b

^a Control System Department, University of Grenoble, France

^b Laboratoire d'Astrophysique de Grenoble, UMR5571 CNRS, Université Joseph Fourier, BP 53, 38041 Grenoble Cedex 9, France

^c European Southern Observatory, Casilla 19001, Santiago 19, Chile

ABSTRACT

Fringe-tracking has long been recognized as a critical system for modern astronomical ground interferometry to stabilise observations. The incoming generation of trackers is intended to co-phase a large number of telescopes simultaneously, bringing new questions related to control and redundancy. In this paper, we propose a new control architecture for the 4/6-telescope Second Generation Fringe Tracker, currently under study for the Very Large Telespoes Interferometer (VLTI). The main feature of the proposed solution lies in the explicit handling of coupling and redundancy. This enables in particular to tune the different baselines control-related weighting coefficients according to the presence of noise and or potential loss of flux. Moreover, the unavoidable delays are explicitly taken into account in the control design while an observer is used to reconstruct the dynamic of the atmospheric OPD. The control design is based on a multi-variable state space representation making possible the use of standard Linear Quadratic design. The resulting controller can still be expressed in a transfer function form. The efficiency of the proposed solution is illustrated through dedicated simulations involving realistic data.

Keywords: VLTI, Fringe tracker, Second Generation, Multi-variable Control, Linear Quadratic

1. INTRODUCTION

The Very Large Telescope (VLT) is one of the most important site for astronomical observation in the world, located at Cerro Paranal in Northern Chile. This ESO's (European Southern Observatory) site is composed of four 8.2m Unit Telescopes (UTs), four 1.8m Auxiliary Telescopes (ATs), an instrumental laboratory, up where the light beams are routed by (currently six) underground delay lines.¹ These telescopes can work together, making the VLT Interferometer (VLTI).

The stellar interferometry allows to improve the angular resolution up to 20 times compared to that of individual telescopes. Indeed, the angular resolution is proportional to $1/B$, where B is the baseline, the projected distance separating the telescopes. Images can be reconstructed with an angular resolution of milliarcsecond. A basic stellar interferometer is made of two telescopes, which collect light from a common target, and an instrument to do interfere the two beam light. The multi-beams interferometry permits to couple N telescopes two-two, and thus to gain observing time. Currently two instruments permit to observe in interferometry : MIDI² (recombines fluxes from two telescopes in thermal infrared) and AMBER³ (recombines three telescopes in near infrared). POPS should operate in near infrared, probably in K band (1.9-2.4 μm). The 2nd Generation VLTI instruments are developing, as GRAVITY⁴ or VSI,⁵ and will recombine 4 to 6 telescopes.

In interferometry from ground, one of the most important limit is the atmospheric turbulence, which introduces a dephasing between beams (Figure 1 left). This Optical Path Difference (OPD) is random and larger than the fringe spacing. Thus the fringes are continuously moving and it becomes impossible to measure the astrophysical observables : the visibility and the phase (Figure 1 right). To resolve this problem, an interferometer need to have a fringe tracker which measures the dephasing and correct it in real-time thanks to the Delay Lines (DLs). At the VLTI, two fringe trackers are operating : FINITO⁶ (three beams fringe tracker) and PRIMA⁶ (two beams fringe tracker off axis).

The 2nd Generation Fringe Tracker (2GFT) is an ESO project to the VLTI. Currently in its phase A study, this fringe tracker will be able to co-phase 4 to 6 telescopes for the new generation instruments. POPS (Planar Optic

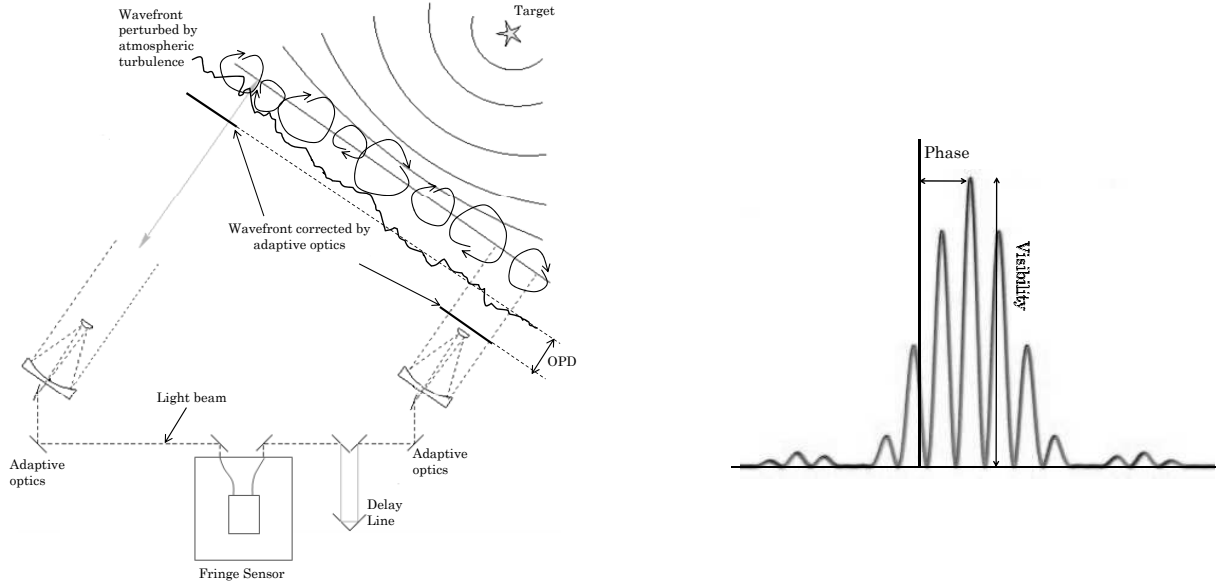


Figure 1. Left : Problematic of the piston OPD. Right : the two observables on interference fringes

Phase Sensor) is the response project led by LAOG. It's in this context that a control loop is studied, but it's not dependant of the technologic choices of POPS, while the input of the loop are the OPD to be corrected. The role of the control loop is to command the N DLs to cophase the fluxes from the N telescope from $N - 1$ to $N(N - 1)/2$ measures of phase. The solution to command each DL with a dedicated controller not seems to be the most judicious because of the coupling of the measures. From a standpoint of control, the eventual redundancies in multi-beam fringe tracking can allow theoretically to track bases unmeasured or too much noised. This paper investigate a coupled solution and show some of its potential advantages. We consider the N DLs like a one global mechanical system controlled from all input measures without to try to indentify which DL permits to act on which measure. The proposed solution use the explicit handling of coupling and redundancy to tune the different baselines control-related weighting coefficients according to the presence of noise and or potential loss of flux.

In section 2, the VLTI basic problem is stated as control equations, the control design of the mechanical system is described in section 3 and some simulations are presented in section 4 to illustrate the operating of the solution.

2. PROBLEM STATEMENT

The interferometry is a phenomenon which appeal to the wave aspect of light. An interferometer recombine two beams from a same target to form an interference pattern, alternation of bright and dark fringes, and which the inter fringe is the wave length. But to see these fringes the two beams need to be coherent, ie the light from the target need to have travel the same length. An Optical Path Difference (OPD) between beams results in a lag of the fringe on the interference pattern. Thus an OPD of one wave length lag the fringe of one inter fringe. Because of the width of the spectral band observed the interference pattern exist only on a defined space of few length wave, and the inter fringe become the average wave length of the spectral band. Thus, if the OPD becomes too important, the fringes are so lagged that they are no longer observable.

The atmospheric turbulence can be shown as air buble of different size and in perpetual moving. A wave front from observed target crosses the air layer above the telescopes and it's perturbed by the turbulence. The perturbed share of the wave front observed by a telecope is (theoretically) corrected by optical system (like Adaptive Optics). But each telescope of the interferometer look through a different share of the air layer. Thus, even if wave fronts are locally corrected, it stay an OPD between them called piston. This OPD varies about several decade μm during few μs . It becomes impossible to do exposure (few μs) to observe the fringe, while

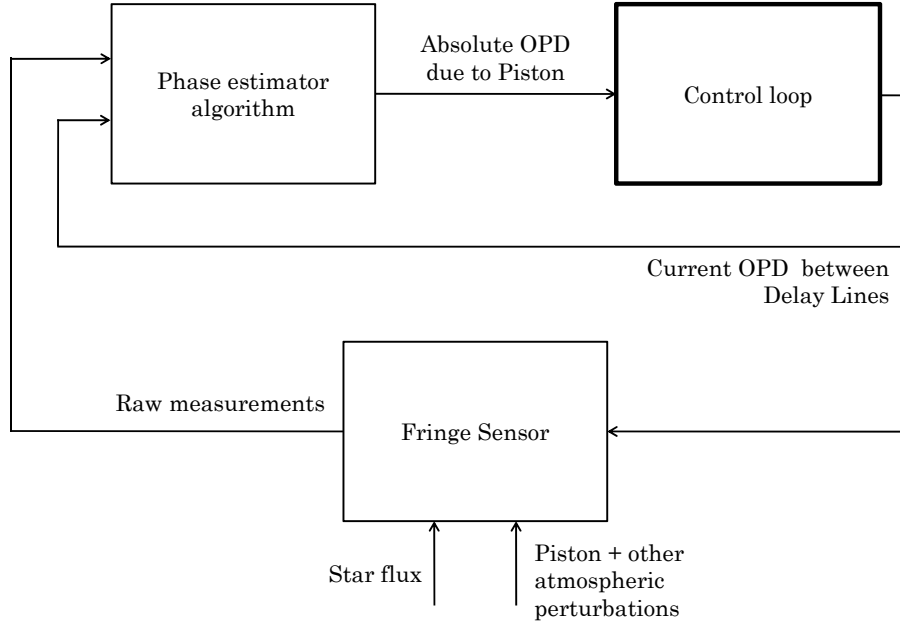


Figure 2. Scheme of a fringe tracker loop

fringe are moving during the exposure time.

The fringe tracker is an interferometer dedicated to measure the phase (reflect of the OPD due to piston) and to compensate it thanks to opto-mechanical system. The fringe sensor and the phase estimator are the parts of the fringe tracker which measure the OPD, while the Control Loop is the part which command the opto-mechanical system (DLs) to compensate the OPD (Figure 2). A Delay Line is a carriage which transports a mirror, on rails (at VLTI the length is about 60m). This system permits to extend the optical path of a telescope beam. Each telescope of the interferometer has a DL along its optical path. Without turbulence, the DLs have to compensate only the well known OPD due to the distance separating the telescopes. But because of the piston they serve also to compensate it. This paper concentrate thus on the control of the DLs to compensate the OPD mesured.

2.1 Mechanical model

The position d_i of the DL i depend of the command U_i applied to it and the specifications of the mechanical system (Eq. 1). The frequency behaviour of the mechanical system can be described as a transfert function (Eq. 2).

$$d_i(s) = T_{DL_i}(s) \cdot U_i(s) \quad (1)$$

$$T_{DL_i}(s) = \frac{130.4s^6 - 1.047 \cdot 10^6 s^5 + 4.273 \cdot 10^9 s^4 - 7.88 \cdot 10^{12} s^3}{s^7 + 6577s^6 + 2.157 \cdot 10^7 s^5 + 6.551 \cdot 10^{10} s^4 + 1.029 \cdot 10^{14} s^3} \quad (2)$$

where s is the Laplace operator.

The Figure 3 shows the bode diagram of this transfert function. The continue compositant (low frequency) is null, thus the control input is the set-point of the system. It's probably already looped and controlled.

If we call d the vector containing the N positions of the N DLs, we can describe the vector Y (Eq. 3), which

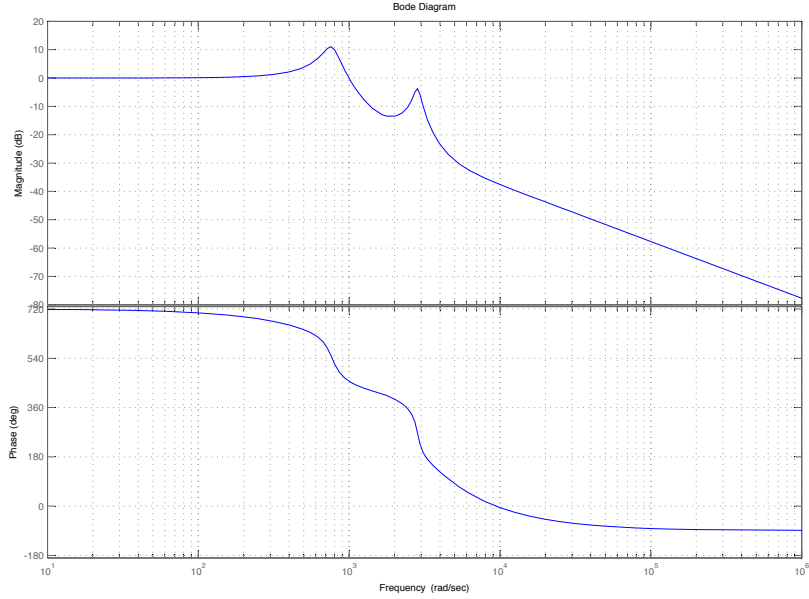


Figure 3. Bode diagram of the transfert function of a DL

contains the $B \in [N - 1; N(N - 1)/2]$ (according to the scheme of recombination choised) OPD measured (thanks to the DLs metrology system) between DLs :

$$Y = M \cdot d \quad (3)$$

where M is the interaction matrix,⁷ completed with 1, -1 and 0, which describes how DLs form what base. The mechanical model of the N DLs, which is our open loop system, can be written as a state representation⁸ :

$$X^+ = A \cdot X + B \cdot U \quad (4)$$

$$Y = M \cdot C \cdot X \quad (5)$$

A , B and C are matrix dependent on the DLs model (that to say dependent on the transfert function). X is the state vector, which contain all states (position, velocity, acceleration, etc) of the DLs (in our case each DL is described by 7 states, so $X \in \mathbb{R}^{7N \times 1}$). In the equation (4), the $+$ represents the next computing instant. U is still the command vector $\in \mathbb{R}^{N \times 1}$ and Y measurement vector $\in \mathbb{R}^{B \times 1}$. We express the output Y in term of OPD because it's the variable to control, in deed we know the input of the future closed loop will be the OPD, due to the piston and measured by the fringe sensor.

2.2 Problematic

The problematic is thus to produce N commands (positions of each DLs) to control B variables (OPD between DLs), potentially dependant each others. The goal of a fringe tracker is to produce, thanks the DLs, an OPD equal to the OPD Piston. From a control stand point, the problematic could be presented as a minimization of a cost function, for example the gap between the OPD Piston (input of the loop) and the OPD DLs (output of the loop). The control could also take in to account the redundancy and dependance of OPD each other, to control DLs with the best input measures by weighting them.

The control loop have to deal with several pathological situations. Because of residual error from the adaptive

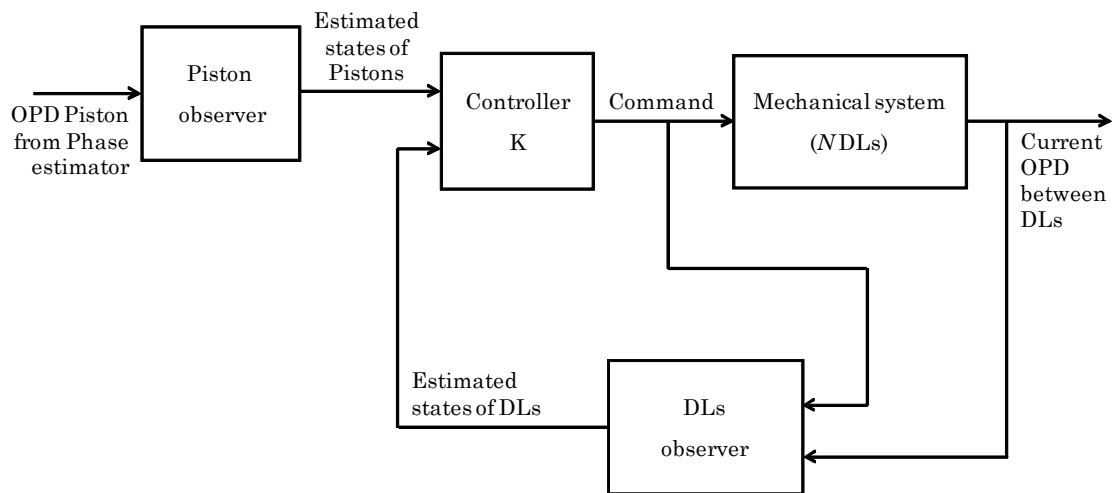


Figure 4. Scheme of control loop

optics (tip/tilt for example), loss of flux from a telescope can occur. It produce an increase of the measurement noise on each OPD due to Piston measures affected by this telescope flux. This noise is random and independant on each bases, thus the B measures become slightly independant each others. No one DLs configuration permit thus to solve the problem, and the consequence is the noise propagation to others bases (while their measures are less noised) through the DLs. More rarely, only one base can be more noised because the baseline is longer than others and resolve the target. But even if the measures are not much noised, the monitoring is difficult because of the pure delay (addition of DIT, computing delay, ...). The control loop is compensating a piston which has occurred long ago. The error between the current OPD due to piston and the OPD between DLs is thus always important.

Because of all this operating constraints and the profile of the system, a multi-variable linear quadratic design⁸ seems to be a suitable answer to this control problematic.

3. THE PROPOSED CONTROL DESIGN

The control loop (Figure 4) describe here is the content of the box "Control loop" on Figure 2. The input of the loop is thus the B OPD due to piston (measured by the fringe sensor and then deliver by the estimator, see Figure 2) and its output is the current OPD between DLs (measured by the DLs metrology system).

As seen in section above, the pure delay kill the performances of the monitoring, even if atmospherical conditions are good. In deed, we undregro this delay and correction are made too late after the real perturbation. It appears, the need to know an estimation of the disturbance dynamic is essential. It should permit to catch up the delayed set point when its dynamic will be stable.

3.1 Observer

To estimate the dynamic of the piston we need an observer.⁸ A state observer estimates states of the system knowing a priori the model (state representation, transfert function, ...), the outputs (measures) and the inputs (command, if the system is controllable) of the system. In deed states of a system are rarely all known because

some can be unmeasured or unmeasurable. In our case the piston is an unknown system and is not controllable (thus there are not inputs). To estimate the first orders of the dynamic of the piston, we suppose its evolution can be constant (knowing of the value only, as there is no observer), linear or quadratic, thus we estimate respectively pu to the zero, first or second order of the dynamic. The state representation of the observer of the B setpoints (OPD due to piston) is :

$$\widehat{Z}^+ = A_z \cdot \widehat{Z} + L_z \cdot (Y_z - \widehat{Y}_z) \quad (6)$$

$$\widehat{Y}_z = C_z \cdot \widehat{Z} \quad (7)$$

where, \widehat{Z} is the estimation of the *rang* (*rang* = order of the model + 1) states of the B pistons, $A_z \in \mathbb{R}^{B.rang \times B.rang}$ and $C_z \in \mathbb{R}^{B \times B.rang}$ the matrix of the piston model (constant, linear or quadratic), Y_z the input pistons of the observer (input of our control loop : OPD due to piston measured) and L_z the observer matrix such as $(\widehat{Y}_z - Y_z) \rightarrow 0$.

We need also a state observer of the mechanical system. The model (Eq. 4 and 5), the input (command) and the output (current OPD between DLs) of this system are well known. We can thus make a classical Kalman observer.⁸ The following representation (Eq. 8 and 9) is the model of the state observer :

$$\widehat{X}^+ = A \cdot \widehat{X} + B \cdot U + L \cdot (Y - \widehat{Y}) \quad (8)$$

$$\widehat{Y} = M \cdot C \cdot \widehat{X} \quad (9)$$

where L is the observer matrix, such as $(\widehat{X} - X) \rightarrow 0$.

3.2 Extended system

The future controller need to take into account the states of the DLs and the pistons. To take into account the pure delay describe section 3, the command is delayed. To simulate it, the matrix A , B , C of the DLs model are modified in A_s , B_s , C_s . Thus we can describe the state representation of the two system (DLs and pistons) in open loop :

$$\begin{pmatrix} X_s^+ \\ Z^+ \end{pmatrix} = \begin{pmatrix} A_s & 0 \\ 0 & A_z \end{pmatrix} \cdot \begin{pmatrix} X_s \\ Z \end{pmatrix} + \begin{pmatrix} B_s \\ 0 \end{pmatrix} \cdot U \quad (10)$$

$$\epsilon = Y_z - Y_s = (-C_s \quad C_z) \begin{pmatrix} X_s \\ Z \end{pmatrix} \quad (11)$$

ϵ is the residual OPD, gap between OPD piston and OPD DLs.

3.3 Controller design

The aim of the controller K is to minimize the residual OPD on a futur time sequence. We name $\tilde{\epsilon}$ the vector containing all errors on this time sequence :

$$\tilde{\epsilon} = \begin{pmatrix} \epsilon^{+1} \\ \epsilon^{+2} \\ \vdots \\ \epsilon^{+N} \end{pmatrix} \quad (12)$$

where N is the number of computing step.

We can thus show $\tilde{\epsilon}$ can be described like a fonction of states and a sequence of command \tilde{U} :

$$\tilde{\epsilon} = \Phi \cdot \begin{pmatrix} X_s \\ Z \end{pmatrix} + \Psi \cdot \tilde{U} \quad (13)$$

where $\tilde{U} = \begin{pmatrix} U \\ U^+ \\ \vdots \\ U^{N-1} \end{pmatrix}$.

To construct the controller, we simplify the problem supposing the command during the time sequence is constant. This choice is done to be able to describe $\tilde{\epsilon}$ like a simple state representation, function of states and a command. Thus the equation (13) can be written :

$$\tilde{\epsilon} = \Phi \cdot \begin{pmatrix} X_s \\ Z \end{pmatrix} + Q\Psi \cdot \Gamma U \quad (14)$$

where $\Gamma = \begin{pmatrix} I \\ I \\ \vdots \\ I \end{pmatrix}$, I the identity matrix $\in \mathbb{R}^{N \times N}$ and $Q \in \mathbb{R}^{B \times B}$ the diagonal matrix containing the weights of each bases according the confidence.

The controller K have to produce the best command U to minimise the cost function $C_U = \tilde{\epsilon}^t \cdot \tilde{\epsilon}$, from given states (estimated states in fact). Thus, we can write the solution of this minimization like a simple state feedback :

$$U = K \cdot \begin{pmatrix} \widehat{X}_s \\ \widehat{Z} \end{pmatrix} \quad (15)$$

$$= \begin{pmatrix} K_1 & K_2 \end{pmatrix} \cdot \begin{pmatrix} \widehat{X}_s \\ \widehat{Z} \end{pmatrix} \quad (16)$$

And the global closed loop system can be written :

$$\begin{pmatrix} X_s^+ \\ Z^+ \\ \widehat{X}_s^+ \\ \widehat{Z}^+ \end{pmatrix} = \begin{pmatrix} A_s & 0 & B_s K_1 & B_s K_2 \\ 0 & A_z & 0 & 0 \\ L_s C_s & 0 & A_s - L_s C_s + B_s K_1 & B_s K_v \\ 0 & L_z C_z & 0 & A_z - L_z C_z \end{pmatrix} \cdot \begin{pmatrix} X_s \\ Z \\ \widehat{X}_s \\ \widehat{Z} \end{pmatrix} \quad (17)$$

In equation (17) the pistons are auto-produced by the model of piston (second line), thus this model has not input. But in simulations the input is the setpoint $Y_z = C_z \cdot Z$. We can rewrite the Equation (17) :

$$\begin{pmatrix} X_s^+ \\ Z^+ \\ \widehat{X}_s^+ \\ \widehat{Z}^+ \end{pmatrix} = \begin{pmatrix} A_s & 0 & B_s K_1 & B_s K_2 \\ 0 & A_z & 0 & 0 \\ L_s C_s & 0 & A_s - L_s C_s + B_s K_1 & B_s K_v \\ 0 & 0 & 0 & A_z - L_z C_z \end{pmatrix} \cdot \begin{pmatrix} X_s \\ Z \\ \widehat{X}_s \\ \widehat{Z} \end{pmatrix} + \begin{pmatrix} 0 \\ 0 \\ 0 \\ L_z \end{pmatrix} \cdot Y_z \quad (18)$$

4. ILLUSTRATIVE EXAMPLES

We present now some Matlab simulations to illustrate the performances of the control loop. On each of the following simulations the current OPD between DLs is plot in broad blue, the setpoint is plotted in black and represents the current absolute OPD due to Piston. The current residual OPD after correction is plotted in thin blue. The total delay simulated is $5ms$ ($4ms$ of DIT and $1ms$ of computing delay) which represents the delay between the moment when the perturbation occurs and that the Control loop receives the measure. The residual OPD RMS is plot on each figures to compare performances.

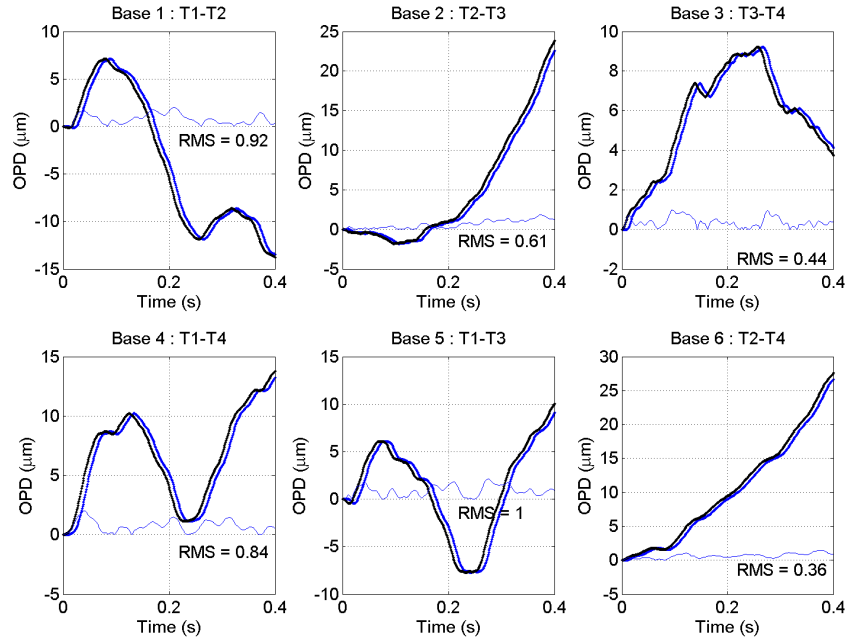


Figure 5. Simulation results with $N = 4$ and $B = 6$. Control loop with piston observer order 0, but no take into account of delay. Black : setpoint (piston); Blue : OPD between DLs; Blue thin : residual OPD

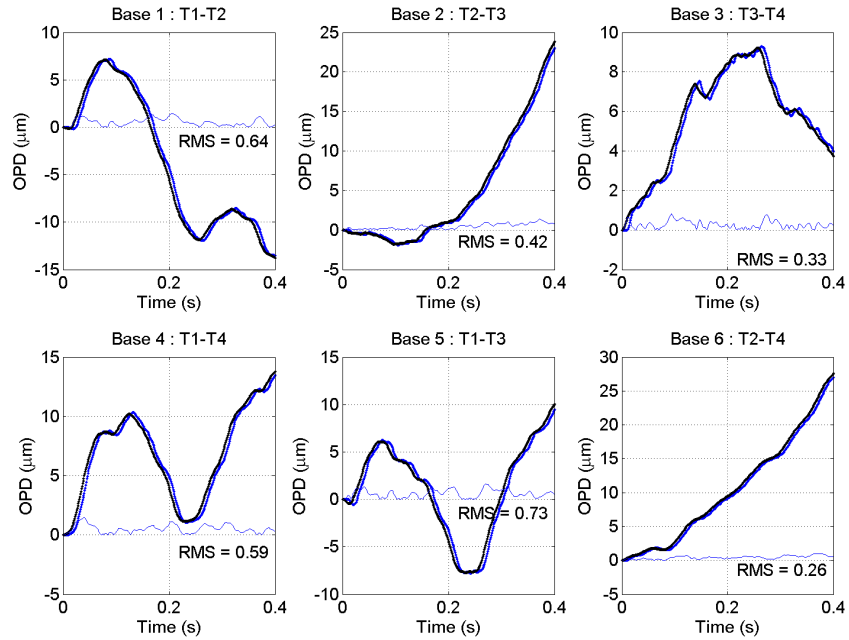


Figure 6. Simulation results with $N = 4$ and $B = 6$. Control loop with piston observer order 1, but no take into account of delay. Black : setpoint (piston); Blue : OPD between DLs; Blue thin : residual OPD

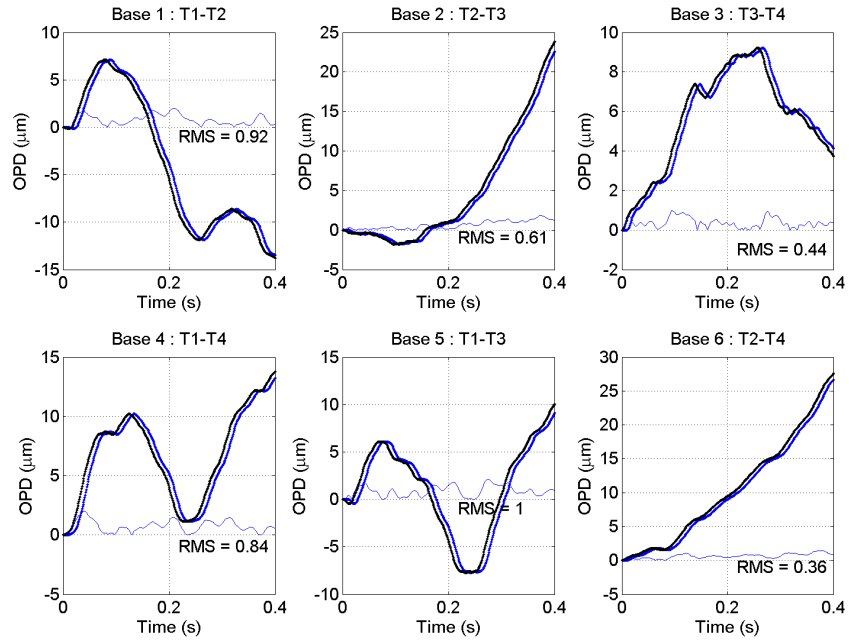


Figure 7. Simulation results with $N = 4$ and $B = 6$. Control loop without piston observer. Black : setpoint (piston); Blue : OPD between DLs; Blue thin : residual OPD

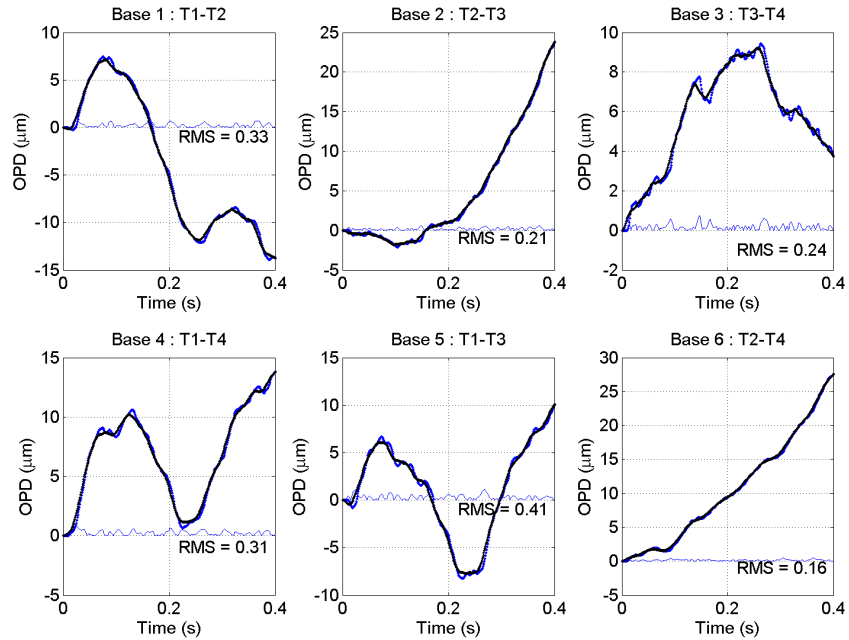


Figure 8. Simulation results with $N = 4$ and $B = 6$. Control loop with piston observer order 1. Black : setpoint (piston); Blue : OPD between DLs; Blue thin : residual OPD

4.1 Effect of the explicit handling of delay and of the observer order

The Figure (5) show results in standard situation, if we don't take into account the delay and the order of the observer is zero (no estimation of the dynamic). The monitoring of the setpoint works good, but with a constant delay, thus generating an important error (residual OPD) . It shows how the performances of the loop in terms of residual OPD is highly limited by the delay of the system, and the need of an observer to estimate the disturbance dynamic.

On Figure (6), the order of the observer is now 1. It estimates the velocity of the piston and thus the delay is slightly compensated, but it remains a constant delay.

The Figures (7) and (8) present the monitoring when the observer is respectively of order 0 and 1 (linear), with take into account of the delay. The first one is same as the Figure (5) because beside the controller know the delay, it don't have enough informations to compensated it.

On the Figure (8), performances are clearly better with observation of dynamic disturbance (Observer order 1), the delay is gradually compensated. The delay is now only sustained when big variations occur, appearing like overtakings. The simulations with an observer of order 2 has been runned but results are sensibly the same.

To compare the performances according of the observer used and the taking into account of the delay for the design of the controller, we can define a score : the *lock ratio* is the proportion of time during which the residual OPD is less than 300nm. The table (1) shows overall performances of the loop :

Table 1. *lock ratio* on each bases for different orders of the piston observer

Bases	Observer of order 0	Observer of order 1	
		No Taking into account of Delay	Taking into account of Delay
1	16.9%	32.4%	63.6%
2	39.6%	45.1%	78.6%
3	43.9%	59.8%	81.5%
4	19.2%	25.7%	59.4%
5	18.5%	27.2%	49.9%
6	14.7%	28.7%	89.5%
Mean	25.5%	36.5%	70.4%

4.2 Pathological operating cases

For the simulation presented section 4.1, we have consider the pistons in inputs like noisefree, thus dependant of each other. In fact, the inputs come from the piston estimator, and thus the measures have an error, a noise measurement, more or less important according especially to photometrics fluxes. The typically problem is due to tip/tilt effect, resulting a drop out (up to loss) on the affected flux and thus on the fringes visibility of the affected bases. Measures are then more noised (up to be only noise is flux is lost) and become independant of each other, since the noise is independent to each bases (Figure (9)). This independance makes the exact DLs configuration which have to compensate the OPD piston impossible to be found, unlike when the pistons are dependant. The monitoring find then a compromise quites to follow the more noised measures, whereas measures from others bases can be less noised, more reliable (first half of simulation on Figure (9) and (10)). We simulate this noise as a Gaussian noise (with null mean and standard deviation given), added to each measure.

But if we have an indicator which reflects the confidence that we have in each measures, it's possible to weight them (thanks to the matrix Q described section 3.3). The weighting allows the controller to take into account the redundancy to minimize the effect of the noise measurement. The indicator which permits that could be the SNR estimated by the Phase Estimator or, like in the simulations below (second half of simulations, Figure (9) and (10)), the standard deviation of a few past input value sequence*.

*To compute the standard deviation of few past input values (7 for the simulations presented), we subtract at each sequences the theoretical linear continuous component, to avoid false noise detection due to strong linear variation of noisefree piston. The weight applied on each bases is thus the inverse of the STD.

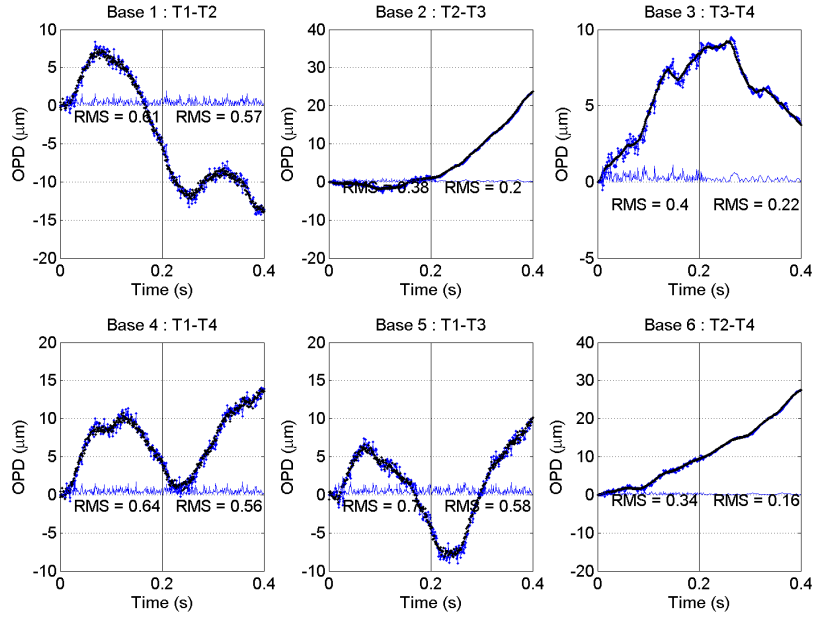


Figure 9. Simulation of a loss of flux from the telescope 1, with $N = 4$ and $B = 6$. Measures from the three bases affected by this telescope are more noised. During the first half the weighting is off, and it's on during the second one. Control loop with piston observer order 3. Black : setpoint (piston); Blue : OPD between DLs; Blue thin : residual OPD

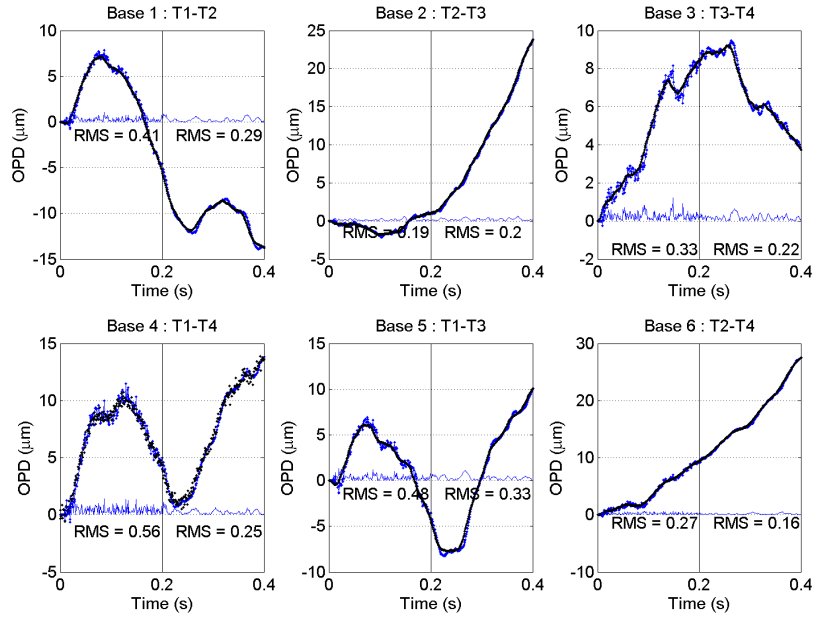


Figure 10. Simulation of a drop out of visibility on the base 4, with $N = 4$ and $B = 6$. Measures from this bases is more noised. During the first half the weighting is off, and it's on during the second one. Control loop with piston observer order 3. Black : setpoint (piston); Blue : OPD between DLs; Blue thin : residual OPD

An other pathological case, rarer, it's a drop out of the fringe visibility on one base. It can appear when a baseline is much larger than others ones and thus it resolves the target. The measurement noise become higher on this base (on Figure (10) the base 4). Although only measures from one base are noised, we can see the noise is propagated to others bases, through the DLs (first half of simulation on Figure (10)). The weighting permits to minimize the impact of the noised base for monitoring, and even in this case, to reconstruct monitoring of the base 4 (second half of simulation on Figure (10)).

5. CONCLUSION AND FUTURE WORK

We have design a control achitecture which permits to co-phase an interferometric telescope network for more than 3 telescopes. The delay has been explicitly taken into account to improve the residual OPD. To do that, an observer of the piston dynamic was developped to estimate the movement of the disturbance. The controller is design on linear quadratic minimisation of the residual OPD. Knowing both the current estimations of DLs states and of the piston dynamic, it produces the best command for DLs to respect this criterion.

In this paper, we also simulate the Control loop of the fringe tracker, assuming the Fringe Sensor and the Phase Estimator are perfect (except delay and noise measurement). The output (OPD between DLs) has not impact on the input (measures from the Fringe sensor) in our simulation, the 2GFT loop is open. It will be necessary to simulate the 2GFT loop closed, to observe the behaviour of the Control loop with others phenomenon like drift. The controller has been design to be easily transformable in a transfer function form, in order to be integrated in a Fringe Tracker simulator.

The N DLs use in simulation are based on the transfert function describe section 2.1 (Eq. 2), but we know each DL are slightly different and thus each one has its transfert function, especially since DLs have been improved. Finally, use hardware system instead of model could be an experimental validation.

REFERENCES

1. Hogenhuis, H. and al., "Commissioning of the vlti delay lines on mount paranal," in [*Interferometry for Optical Astronomy II*], Traub, W. A., ed., *Proc. SPIE* **4838**, 1148–1154 (2003).
2. Hippler, S. and al., "Midi : controlling a two 8-m telescope michelson interferometer for the thermal infrared," in [*Interferometry in Optical Astronomy*], Lena, P. and Quirrenbach, A., eds., *Proc. SPIE* **4006**, 92–98 (2000).
3. Malbet, F. and al., "Astrophysical potential of the amber/vlti instrument," in [*Interferometry for Optical Astronomy II*], Traub, W. A., ed., *Proc. SPIE* **4838**, 917–923 (2003).
4. Eisenhauer, F. and al., "Gravity : The ao-assisted, two-object beam-combiner instrument," in [*The Power of Optical/IR Interferometry: Recent Scientific Results and 2nd Generation VLTI Instrumentation*], Paresce, F., Richichi, A., Chelli, A., and Delplancke, F., eds., *Proceedings of the ESO Workshop* (2005).
5. Malbet, F. and al., "Vsi : a milli-arcsec spectro-imager for the vlti," in [*Advances in Stellar Interferometry*], Monnier, J. D., Schller, M., and Danchi, W. C., eds., *Proc. SPIE* **6268** (2006).
6. Gai, M. and al., "The vlti fringe sensors : Finito and prima fsu," in [*New Frontiers in Stellar Interferometry*], Traub, W. A., ed., *Proc. SPIE* **5491**, 528 (2004).
7. Blind, N., "Suivi de franges : stratgies de recombinaison," *Internal Memo* (2009).
8. Kwakernaak, H., [*Linear optimal control systems*], Wiley-interscience (1872).